Available online at www.sciencedirect.com
ScienceDirect
Journal of Solid State Chemistry 180 (2007) 360–369
JOURNAL OF SOLID STATE CHEMISTRY
www.elsevier.com/locate/jssc

Rapid communication

Structural evolution of $(Ca_{0.35}Sr_{0.65})TiO_3$ perovskite at high pressures

Michael A. Carpenter[a,*], Susana Rios[b], Peter Sondergeld[a], Wilson Crichton[c], Pierre Bouvier[d]

[a]*University of Cambridge, Department of Earth Sciences, Downing Street, Cambridge CB2 3EQ, UK*
[b]*Departmento Física de la Materia Condensada, Facultad de Ciencia y Tecnología, Universidad del País Vasco, Apdo. 644, 48080 Bilbao, Spain*
[c]*ESRF, 6 Rue Jules Horowitz, BP 220, 38043 Grenoble CEDEX 9, France*
[d]*LEPMI-ENSEEG, 1130 Rue de la piscine, B.P. 75, 38042 St. Martin d'Hères, France*

Received 12 June 2006; received in revised form 25 September 2006; accepted 26 October 2006
Available online 28 October 2006

Abstract

Lattice parameters of a synthetic powder sample of $Ca_{0.35}Sr_{0.65}TiO_3$ perovskite have been determined by the method of Le Bail refinement, using synchrotron X-ray diffraction patterns collected at pressures up to 15.5 GPa with a membrane-driven diamond anvil cell. At ambient conditions, diffraction data were consistent with the $I4/mcm$ structure reported previously in the literature for the same composition. Diffraction data collected at high pressures were consistent with tetragonal (or, at least, pseudo-tetragonal) lattice geometry, and no evidence was found for the development of any of the orthorhombic structures identified in other studies of (Ca, Sr)TiO_3 perovskites. Additional weak reflections, which could not be accounted for by the normal $I4/mcm$ perovskite structure, were detected in diffraction patterns collected at pressures of 0.9–2.5 GPa, and above ~13.5 GPa, however. Small anomalies in the evolution of unit cell volume and tetragonal strain were observed near 3 GPa, coinciding approximately with breaks in slope with increasing pressure of bulk and shear moduli for a sample with the same composition which had previously been reported. The anomalies could be due either to new tetragonal ↔ tetragonal/pseudo-tetragonal phase transitions or to subtle changes in compression mechanism of the tetragonal perovskite structure.

Keywords: Phase transitions; (Ca, Sr)TiO_3; Perovskite; Landau theory; High pressure; Spontaneous strain

1. Introduction

Perovskites from the $Ca_xSr_{1-x}TiO_3$ solid solution have attracted interest for the diversity of structural states and phase transitions which they display in response to changing temperature and composition [1–23]. At high temperatures the stable structure across the entire solid solution is cubic ($Pm\bar{3}m$). The first octahedral tilting instability with falling temperature is then associated with the R point of the Brillouin zone. The resulting superstructure has been widely reported to have $I4/mcm$ symmetry [5,8–10,13,16,20,24–27], though an alternative $Pm\bar{3}m \leftrightarrow Imma$ transition has been suggested for compositions $0.06 \leqslant x \leqslant 0.35$ [18,19,21,22]. Ca-rich samples undergo a further $I4/mcm \leftrightarrow Pnma$ transition, which involves coupling of M and R point octahedral tilt systems [9,13–15,25–27]. Sr-rich samples ($0.12 \leqslant x \leqslant 0.41$) do not undergo the same coupled tilting transition but, rather, transform to an antiferroelectric structure with space group $Pbcm$ [1,10–12,16,19,21,22,28,29]. A recent suggestion is that intermediate compositions might in fact be monoclinic at room temperature [23]. At low temperatures ($\leqslant 35$ K), samples with the $I4/mcm$ structure in the composition range $0.002 \leqslant x \leqslant 0.12$ transform to a ferroelectric structure which is believed to have local symmetry corresponding to point group $mm2$ [4].

All the experimental data from in situ studies at high temperatures and from observations of lattice parameters as a function of composition at room temperature indicate that the $Pm\bar{3}m \leftrightarrow I4/mcm$ transition is accompanied by a small reduction in volume (negative volume strain) [13]. As a consequence, the tetragonal structure is stabilised with respect to the cubic structure by increasing pressure. The transition pressure, P_c, of $SrTiO_3$ is ~6 GPa [30–35], but reduces with increasing Ca-content to 1 bar at $x \approx 0.08$.

*Corresponding author. Fax: 44 1223 333450.
E-mail address: mc43@esc.cam.ac.uk (M.A. Carpenter).

0022-4596/$ - see front matter © 2006 Elsevier Inc. All rights reserved.
doi:10.1016/j.jssc.2006.10.022

A negative volume strain for tetragonal↔orthorhombic transitions is also suggested by a single-crystal diffraction study on a sample with $x \approx 0.35$ which was reported to have $I4/mcm$ symmetry at ambient conditions and $Pnma$ symmetry at 3.5 GPa [36]. All the orthorhombic structures have order parameter components associated with at least two different structural instabilities, however, and it is not necessarily the case that these will couple with strain in the same way. In principle, the M and R point tilting instabilities might both be associated with positive volume strains or both with negative volume strains. Alternatively, one might be positive and the other negative. Add to this the possibilities of volume strains with different signs accompanying antiferroelectric or ferroelectric transitions, and it is apparent that the diversity of structures with increasing pressure could be at least as rich as the diversity found with changing temperature. High pressures might stabilise tilted systems, ferroelectric or antiferroelectric systems, or some new combination of these.

The objective of the present study was to explore the structural evolution with increasing pressure of an intermediate phase in the $Ca_xSr_{1-x}TiO_3$ solid solution by synchrotron X-ray powder diffraction. The composition $x = 0.35$ was chosen because at ambient conditions it lies only ~5 K above the $I4/mcm \leftrightarrow Pbcm$ transition, according to the data of Ranjan and Pandey [11], and because a sample with the same nominal composition had already been reported to undergo a transition $I4/mcm \leftrightarrow Pnma$ somewhere between 0 and 3.5 GPa [36]. In a separate study, variations of bulk and shear moduli have been measured at high pressures by pulse-echo ultrasonic methods using a sample with the same composition [37]. These do not show discontinuities which would be indicative of discrete phase transitions, but they do show subtle anomalies suggestive of an unusual response of the perovskite structure to applied pressure.

2. Experimental methods

2.1. Sample preparation

The sample of perovskite with nominal composition $(Ca_{0.35}Sr_{0.65})TiO_3$ was synthesised following essentially the method as used by Ball et al. [6]. Ca and Sr nitrates were dissolved in water and mixed with Ti-isopropoxide. The resulting gel-like material was dried, ground and calcined. The product was ground in an agate ball mill and then subjected to three further firing and grinding cycles. The first firing was for 36 h at 1350 °C, the second for 12 h at 1600 °C and the third for 36 h at 1600 °C. The sample was finally disaggregated in the ball mill at a slower speed than had been used for intermediate grinding stages (300 rpm instead of 600 rpm). The resulting pale cream powder gave sharp peaks due to perovskite in a standard room temperature X-ray powder diffraction pattern. One barely detectable peak corresponding to a d-spacing of ~3.23 Å was observed, indicating the presence of a trace amount of rutile as an impurity phase. The Ca:Sr ratio of a sintered fragment of the sample was checked on a Cameca SX-100 electron microprobe but an independent determination of the oxygen content has not been obtained.

2.2. High-pressure diffraction data collection

X-ray diffraction data were collected in situ at high pressures using the ID27 high-pressure beam line at the ESRF, Grenoble [38]. The powder sample was loaded into a Le Toullec type membrane-driven diamond anvil cell [39], together with several grains of ruby for pressure calibration and a 4:1 methanol/ethanol mixture as the pressure medium. Diffraction patterns were collected as a function of increasing pressure at room temperature using monochromatic X-rays ($\lambda = 0.3738$ Å). The pressure cell was allowed to relax for 30 min at each pressure and the exposure time for each spectrum was 30 s. A final spectrum was collected at 0.66 GPa during decompression from the maximum pressure of 15.5 GPa. Two-dimensional diffraction patterns obtained with a MAR345 image plate were corrected for geometric distortions using the Fit2D programme [40]. These were subsequently integrated to give conventional intensity versus 2θ angle patterns. Pressure was calibrated using the ruby fluorescent method [41], and was determined in situ in the beamline immediately before and after data collections. This procedure is believed to give a precision of ± 0.05 GPa for the pressures quoted below.

2.3. Refinements

Lattice parameters were determined from each powder diffraction pattern by the Le Bail method [42], using the refinement programme FullProf [43]. Values of tetragonal lattice parameters given by Yamanaka et al. [36] for a single crystal of $(Ca_{0.35}Sr_{0.65})TiO_3$ at ambient conditions were used for the initial trial values when fitting the pattern collected from the loaded but unpressurised cell. In the first cycles of refinement, lattice parameters and a linear baseline were allowed to vary under space group $I4/mcm$. Peak shapes were held fixed with rather narrow widths. In the second set of cycles, the refined lattice parameters were kept fixed and four line shape parameters were allowed to vary. In the final cycles, both the lattice parameters and line shape parameters were allowed to vary. Peak shapes were treated as mixed Gaussian–Lorentzian, with a single value of the mixing proportions (independent of 2θ) and width parameters, u, v, w. These describe the full-width at half-maximum height, FWHM, according to [43]

$$\mathrm{FWHM}^2 = u\tan^2\theta + v\tan\theta + w. \quad (1)$$

Initial values of lattice parameters for refinements of data collected at progressively higher pressures were taken as the refined values from the previous pressure.

An alternative sequence of refinements was also tried, in which u, v and w parameters were taken from refinement of

a diffraction pattern collected at high pressures and then used, unchanged, in all subsequent fitting. This led to essentially the same results in terms of lattice parameters and overall fit parameters. Standard Rietveld refinements of atomic positional parameters were also attempted but these quickly showed that the intensity data, particularly for weak superlattice reflections, are not of sufficient quality to yield reliable results.

3. Results

The complete set of powder diffraction patterns is shown as a stack in Fig. 1, and Le Bail fits to two patterns are shown in Fig. 2. Peaks in the ambient pressure spectrum can be accounted for by tetragonal perovskite, ruby and a trace of rutile; these can all be followed to higher pressures. Values of the conventional Rietveld refinement parameters R_p, R_{wp}, R_e generally fall in the range 8–10%, while χ^2 values were between 1 and 2. Values of the R parameters appear to be slightly higher for refinements of data collected in the pressure range 1–2.5 GPa, however (Fig. 3a). Fig. 3b shows variations of FWHM values, as calculated for different diffraction angles with refined values of the linewidth parameters (Eq. (1)). There seems to be little systematic increase in line broadening with

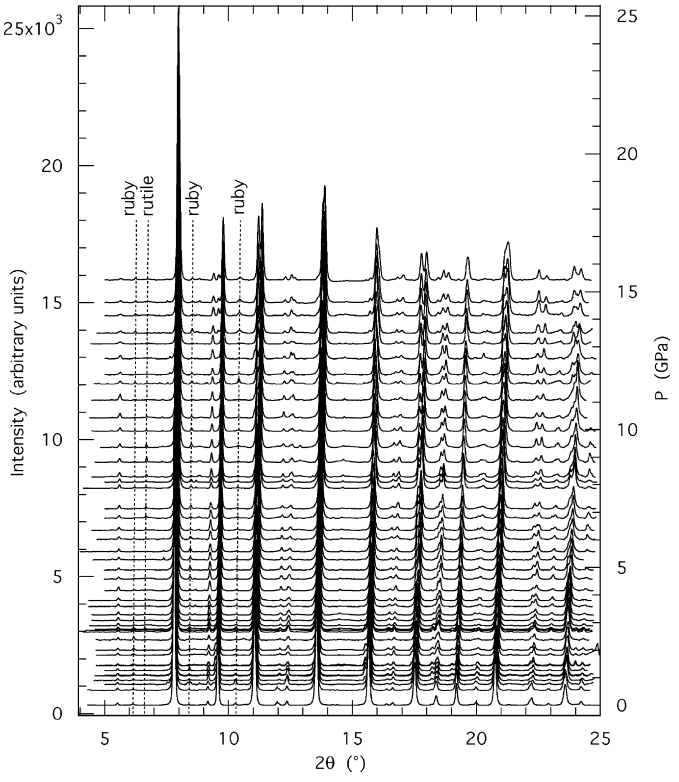

Fig. 1. Intensity in arbitrary units (a.u.) vs. 2θ diffraction patterns for $(Ca_{0.35}Sr_{0.65})TiO_3$ perovskite from two dimensional spectra collected in-situ at pressures up to 15.5 Gpa. *Y*-axis shifts have been applied to all the spectra so that the position of their baselines with respect to the right hand axis gives the approximate pressure at which each one was collected. The diffraction pattern at 0.658 GPa was collected during decompression.

increasing pressure that might be indicative of non-hydrostatic stress up to the solidification point of the methanol:ethanol mixture (~10 GPa, Ref. [44]). On the other hand, there may be a small and relatively abrupt increase in linewidths at about 3 GPa, which is within the range of pressures at which hydrostatic conditions are expected to prevail. Refined lattice parameters obtained from the ambient pressure diffraction pattern, $a = 5.4822(1)$, $c = 7.7891(3)$ Å, are close to values given by Ball et al. [6] for a sample with the same nominal composition, $a = 5.482$, $c = 7.787$ Å, but differ significantly from the single-crystal values given by Yamanaka et al. [36], $a = 5.480(1)$, $c = 7.762(1)$ Å in their Table 1 and $a = 5.473(6)$, $c = 7.742(9)$ Å in their Table 3.

Qualitative inspection of the diffraction patterns suggests that intensities and peak positions vary smoothly with increasing pressure. This is illustrated in Fig. 4a for {0 0 8} and {4 4 0} peaks in the vicinity of $2\theta = 22.5°$. Close inspection of some of the diffraction peaks revealed small, occasional anomalies in peak shapes, such as shown by the {0 0 8}/{4 4 0} doublet at 6.4 GPa and the {4 0 4} peak at 12.06 GPa (Fig. 4). These irregularities were found to be artefacts introduced when converting two-dimensional diffraction patterns into one-dimensional patterns, due to saturation effects. Additional peaks which have not been accounted for by ruby, perovskite or rutile are present in diffraction patterns collected at high pressures, however. These are indicated by arrows at ~9.5°, 15.5° and 19.0° 2θ in Figs. 4b–d. Another similar peak occurs at ~24.0° 2θ. The extra reflections are weak and their shapes vary somewhat irregularly, but they are clearly present at pressures between 0.9 and 2.5 GPa. They are not obviously present at intermediate pressures but the first three, at least, reappear with slightly higher diffraction angles at pressures above 13.5 GPa. Attempts to fit the diffraction patterns using the alternative unit cells of *Pnma*, *Pbcm*, *Imma* and *Cmcm* structures failed to account for these additional weak peaks. The *Pbcm* structure, in particular, may be ruled out on the basis that characteristic superlattice reflections observed at 2θ angles of 37.0, 55.8 and 61.3° in Cu$K\alpha$ patterns [10,12,14,21], have not been observed at the corresponding positions ($2\theta = 8.8$, 13.0, 14.2°) for $\lambda = 0.3738$ Å. Tetragonal↔orthorhombic transitions as a function of temperature in (Ca, Sr)TiO_3 perovskites occur over a narrow (~20–30 K) interval in which the two structure types coexist [22]. Attempts to account for the additional weak peaks as being due to the presence of a second, orthorhombic structure coexisting with the high-pressure tetragonal structure were also not successful, however.

Pseudo-cubic ($a/\sqrt{2}$, $c/2$, $V/4$) values of the tetragonal unit cell parameters are displayed in Fig. 5. These show distinctly non-linear variations with pressure but no major discontinuities. Non-hydrostatic stresses due to solidification of the pressure medium could have been a contributing factor to the non-linear evolution at high pressures, either directly through the effects of shear stress on the sample or

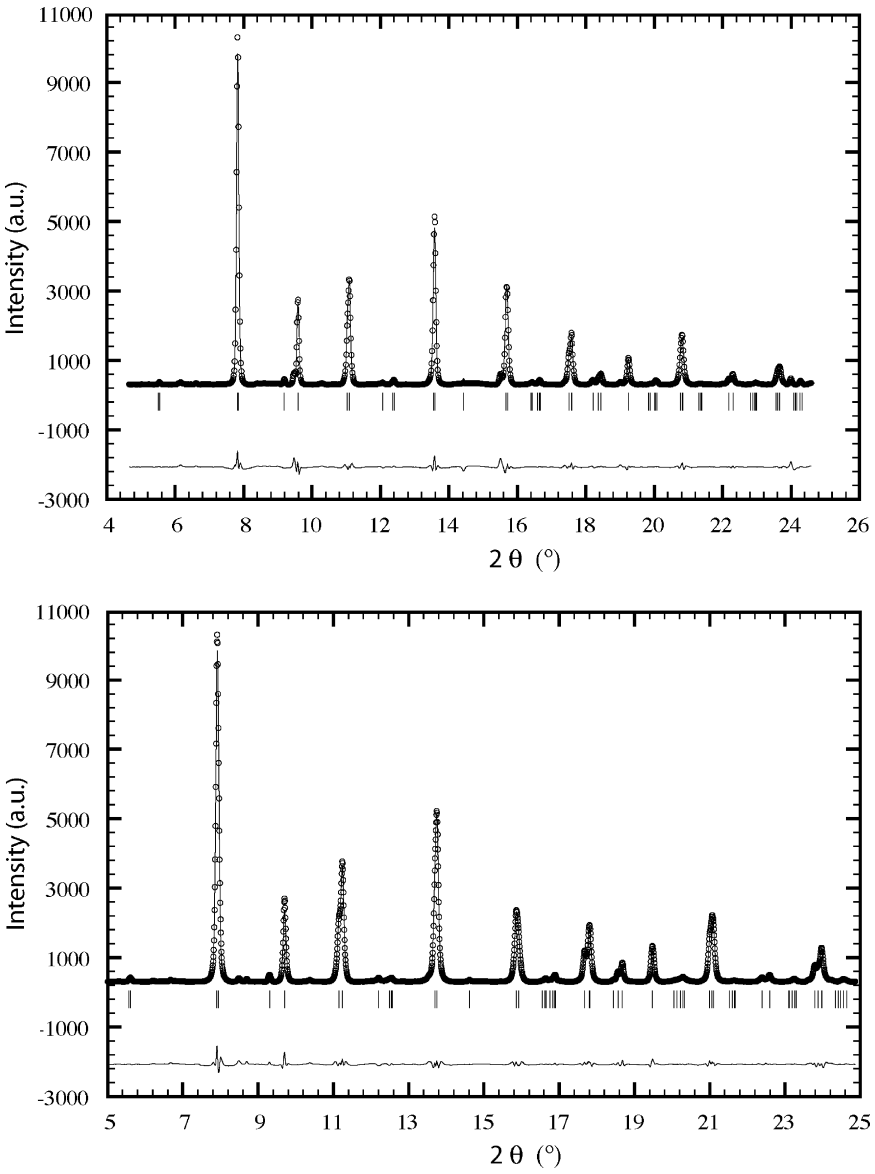

Fig. 2. Outputs from the refinement programme FullProf [43], showing the results of Le Bail refinements under $I4/mcm$ symmetry for diffraction patterns collected at 1.46 (top) and 8.14 GPa (bottom). Vertical lines represent the calculated positions of peaks. The wavy line is the difference between observed and calculated intensities.

indirectly through the effect on ruby pressure calibration. There is, perhaps, a small discontinuity in volume at ~1 GPa, a break in slope in $c/2$ at ~3.5 GPa and a small discontinuity in each of $a/\sqrt{2}$ and $c/2$ at ~13 GPa. These anomalies are barely greater than the scatter in the data, however. Single-crystal data from Yamanaka et al. [36] have been added for comparison but show a quite different, pseudo-cubic trend.

4. Strain analysis

Spontaneous strains which arise at cubic to tetragonal and orthorhombic transitions associated with the M and R points of the Brillouin zone can be analysed using a standard Landau free energy expansion of the form [13,45]:

$$
\begin{aligned}
G = {} & \frac{1}{2}a_1\Theta_{s1}\left(\coth\left(\frac{\Theta_{s1}}{T}\right) - \coth\left(\frac{\Theta_{s1}}{T_{c1}}\right)\right)(q_1^2+q_2^2+q_3^2) \\
& + \frac{1}{2}a_2\Theta_{s2}\left(\coth\left(\frac{\Theta_{s2}}{T}\right) - \coth\left(\frac{\Theta_{s2}}{T_{c2}}\right)\right)(q_4^2+q_5^2+q_6^2) \\
& + \frac{1}{4}b_1(q_1^2+q_2^2+q_3^2)^2 + \frac{1}{4}b_1'(q_1^4+q_2^4+q_3^4) \\
& + \frac{1}{4}b_2(q_4^2+q_5^2+q_6^2)^2 + \frac{1}{4}b_2'(q_4^4+q_5^4+q_6^4) \\
& + \frac{1}{6}c_1(q_1^2+q_2^2+q_3^2)^3 + \frac{1}{6}c_1'(q_1q_2q_3)^2 \\
& + \frac{1}{6}c_1''(q_1^2+q_2^2+q_3^2)(q_1^4+q_2^4+q_3^4) \\
& + \frac{1}{6}c_2(q_4^2+q_5^2+q_6^2)^3 + \frac{1}{6}c_2'(q_4q_5q_6)^2
\end{aligned}
$$

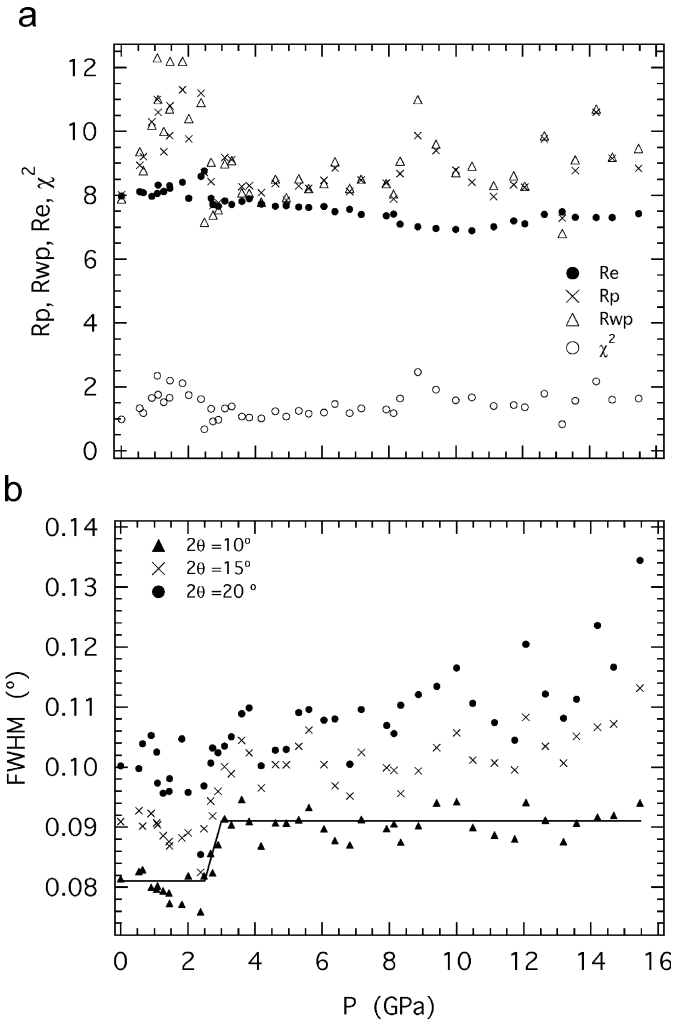

Fig. 3. (a) Variations of the standard Rietveld refinement parameters R_p, R_{wp}, R_e and χ^2 suggest that the quality of fits under $I4/mcm$ symmetry may be slightly worse in the pressure interval 0.9–2.5 GPa than at other pressures. (b) Variations of linewidths calculated for different diffraction angles using Eq. (1) and values of u, v, w obtained from Le Bail refinements. There is very little systematic increase in linewidth with increasing pressure apart, perhaps, from in the vicinity of 3 GPa; lines through the data for $2\theta = 10^\circ$ are guides to the eye to illustrate this point.

$$
\begin{aligned}
&+\frac{1}{6}c_2''(q_4^2+q_5^2+q_6^2)(q_4^4+q_5^4+q_6^4)\\
&+\lambda_q(q_1^2+q_2^2+q_3^2)(q_4^2+q_5^2+q_6^2)\\
&+\lambda_q'(q_1^2q_4^2+q_2^2q_5^2+q_3^2q_6^2)+\lambda_1 e_a(q_1^2+q_2^2+q_3^2)\\
&+\lambda_2 e_a(q_4^2+q_5^2+q_6^2)+\lambda_3[\sqrt{3}e_{oz}(q_2^2-q_3^2)\\
&+e_{tz}(2q_1^2-q_2^2-q_3^2)]+\lambda_4[\sqrt{3}e_{oz}(q_5^2-q_6^2)\\
&+e_{tz}(2q_4^2-q_5^2-q_6^2)]+\lambda_5(e_4q_4q_6+e_5q_4q_5+e_6q_5q_6)\\
&+\lambda_6(q_1^2+q_2^2+q_3^2)(e_4^2+e_5^2+e_6^2)\\
&+\lambda_7(q_1^2e_6^2+q_2^2e_4^2+q_3^2e_5^2)+\frac{1}{4}(C_{11}^o-C_{12}^o)(e_o^2+e_t^2)\\
&+\frac{1}{6}(C_{11}^o+2C_{12}^o)e_a^2+\frac{1}{2}C_{44}^o(e_4^2+e_5^2+e_6^2). \qquad (2)
\end{aligned}
$$

The order parameter components, q_1-q_3, refer to the M point instability while q_4-q_6 refer to the R point instability; a, b, c, etc., are standard Landau coefficients, Θ_{s1} and Θ_{s2} are saturation temperatures, λ_1, λ_2, etc., are strain/order parameter coupling coefficients and C_{ik}^o are elastic constants of the parent cubic structure. The spontaneous strains e_4, e_5 and e_6 are shear strains while, e_a, e_{tz} and e_{oz} are symmetry-adapted combinations of the linear strain components, e_1, e_2, e_3, as

$$e_a = (e_1+e_2+e_3), \qquad (3)$$

$$e_{tz} = \frac{1}{\sqrt{3}}(2e_3-e_1-e_2), \qquad (4)$$

$$e_{oz} = (e_1-e_2). \qquad (5)$$

Here e_a is the volume strain, e_{tz} a tetragonal strain with e_3 in the direction of the unique crystallographic direction and e_{oz} the corresponding orthorhombic strain. Each of e_1, e_2 and e_3 is determined in the usual way from lattice parameter data using an expression of the form $(x-a_o)/a_o$, where x is the pseudo-cubic parameter of the low symmetry structure parallel to reference axes X, Y and Z, and a_o is the reference parameter of the cubic structure. Numerical values of the volume strain are highly sensitive to the choice of a_o, which is usually obtained by extrapolation from the stability field of the cubic structure. In the present study, a cubic structure was not encountered and, therefore, values of e_a cannot be determined. On the other hand, values of e_{tz} are insensitive to the choice of a_o and can be obtained without introducing significant error by assuming $a_o = V^{1/3}$, where V is the pseudo-cubic unit cell volume. The variation of e_{tz} as a function of pressure, as calculated on this basis, is shown in Fig. 6. The shear strains e_4–e_6 are all zero for a tetragonal structure.

The effect of pressure, P, can be introduced into Eq. (2) by adding a term Pe_a. The evolution of the order parameter for a structure with $I4/mcm$ symmetry ($q_4 \neq 0$, $q_1 = q_2 = q_3 = q_5 = q_6 = 0$) is then expected to evolve with pressure according to [46]

$$q_4^2 = \frac{-(b_2^*+b_2'^*)+\sqrt{(b_2^*+b_2'^*)^2+4\frac{2\lambda_2}{\frac{1}{3}(C_{11}^o+2C_{12}^o)}(c_2+c_2'')(P-P_c)}}{2(c_2+c_2'')}. \qquad (6)$$

The critical pressure, P_c, is also the equilibrium transition pressure if the $Pm\bar{3}m \leftrightarrow I4/mcm$ transition is thermodynamically continuous. It is given by [46]

$$P_c = \frac{a_2\Theta_{s2}\frac{1}{3}(C_{11}^o+2C_{12}^o)}{2\lambda_2}\left(\coth\left(\frac{\Theta_{s2}}{T}\right)-\coth\left(\frac{\Theta_{s2}}{T_{c2}}\right)\right). \qquad (7)$$

The tetragonal strain is expected to scale with the order parameter according to

$$e_{tz} = -\frac{2\lambda_4 q_4^2}{\frac{1}{2}(C_{11}^o-C_{12}^o)}. \qquad (8)$$

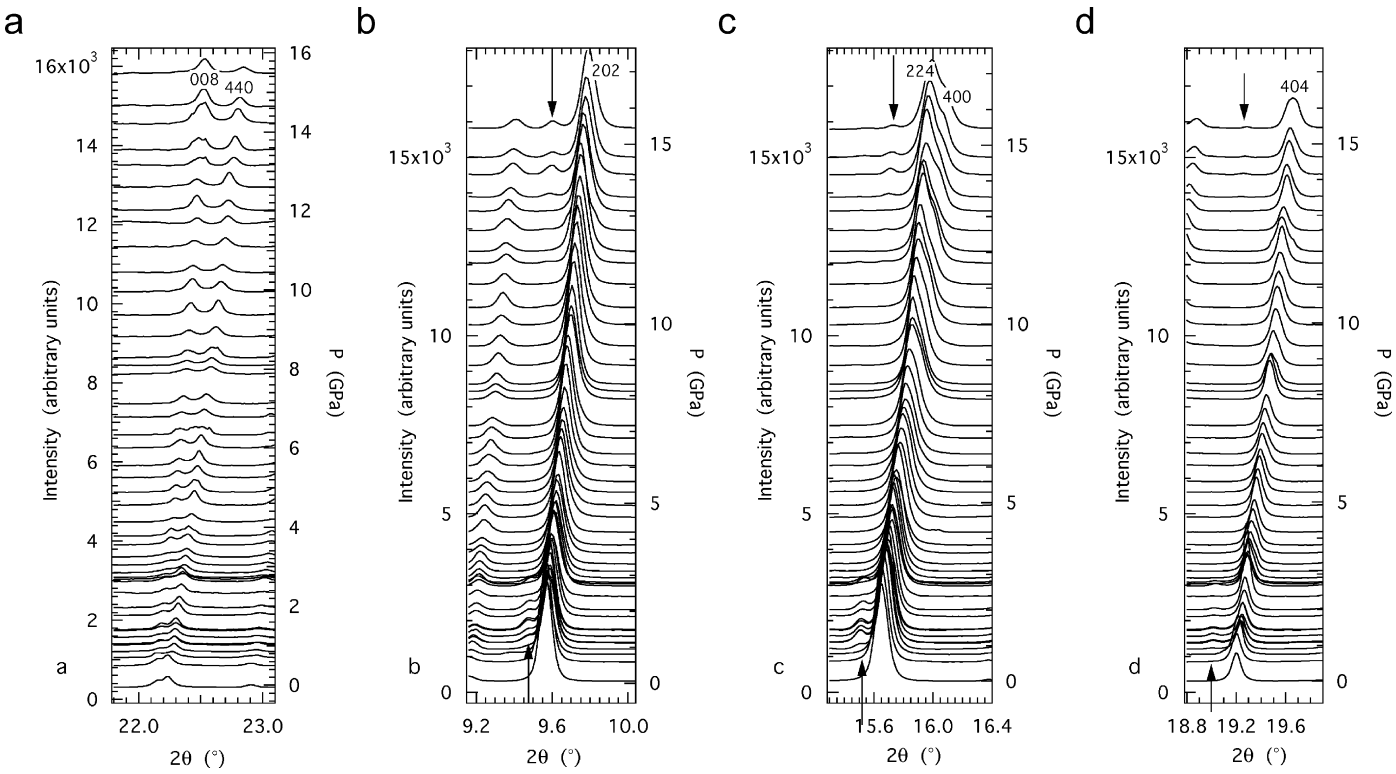

Fig. 4. Selected ranges of 2θ from the stack of diffraction patterns shown in Fig. 1. (a) {0 0 8} and {4 4 0} (tetragonal) reflections (the latter is at higher 2θ) show apparently continuous variations in diffraction angles for the entire pressure interval over which data were collected. (b–d) Additional weak reflections not accounted for by the $I4/mcm$ perovskite structure (indicated by arrows) are present in diffraction patterns collected at 0.9–2.5 GPa and $P \geqslant 13.5$ GPa.

Clearly the tetragonal distortion and, hence, q_4^2 of the sample used in the present study increases with pressure. A linear fit to the data, as shown in Fig. 6, would imply a second-order transition with an extrapolated value of $P_c = -8.41$ GPa. Using $a_2 = 0.000018\,\text{GPa K}^{-1}$, $\Theta_{s2} = 60.8$ K and $\frac{1}{3}(C_{11}^o + 2C_{12}^o) = 180$ GPa determined for the same transition in $SrTiO_3$ [45] and a transition temperature at zero pressure of 722 K (extrapolated between data points taken from the literature and summarised in [46]) gives $\lambda_2 = 0.082$ GPa for $T = 295$ K in Eq. (7). This is slightly greater than the value of $\lambda_2 = 0.046$ estimated for $SrTiO_3$ [45]. If the $Pm\bar{3}m \leftrightarrow I4/mcm$ transition is in fact intermediate in character between second order and tricritical, as appears to be the case for the transition driven by changing temperature [43–47], a non-linear fit to the data in Fig. 6 would be more appropriate, giving a larger (less negative) value of P_c.

Results for e_{tz} as a function of pressure show deviations from the linear fit in Fig. 6 which are greater than experimental uncertainties propagated from the Le Bail refinements. In particular, there appears to be a break of slope in the vicinity of ~3–4 GPa. A transition from $I4/mcm$ to *Imma* or *Pnma* symmetry can be ruled out by considering the discontinuity in tetragonal strain which would be expected to occur but is not observed. M and R point transitions in perovskites have six separate order parameter components (Eq. (2)). Relationships between these and tetragonal strains are listed in Table 1 [13,45,48]. The relevant tetragonal strain for *Imma* and *Pnma* structures, e_{tx}, has b as the doubled cell dimension (which is parallel to reference axis X for the internally consistent set of axes used in the group theory programme ISOTROPY [49]). *Pnma* structures of $Ca_xSr_{1-x}TiO_3$ perovskites have $e_{tx} \approx 0$, because the two tilt systems give rise to strains which are opposite in sign and approximately equal in magnitude. *Imma* structures must have a tetragonal strain which is opposite in sign (pseudo-cubic $b <$ pseudo-cubic $a \approx$ pseudo-cubic c) from the tetragonal strain of $I4/mcm$ structures (pseudo-cubic $c >$ pseudo-cubic $a =$ pseudo-cubic b). Thus $I4/mcm \leftrightarrow Pnma$ and $I4/mcm \leftrightarrow Imma$ transitions should be accompanied by large and abrupt discontinuities in the tetragonal strain, e_t. Such discontinuities are evident, for example, in strain data for CST perovskites [11,50], in lattice parameter data for $Ca_{0.43}Sr_{0.57}TiO_3$ [22] and $SrZrO_3$ [51], and in strain data for the $R\bar{3}c \leftrightarrow Imma$ transition in $PrAlO_3$ at low temperatures [48]. Transformation to a *Cmcm* structure could give the slight change in trend of e_{tz} by the introduction of a small M component tilt (q_3). No direct evidence of this structure has been obtained from the diffraction patterns, however. An equivalent treatment of strains accompanying a transition to *Pbcm* symmetry will require an analysis of the symmetry of strain/order parameter coupling, but the appearance of this structure as a function of temperature is already known to be marked by an abrupt change from tetragonal (or pseudo-tetragonal) lattice geometry to pseudo-cubic geometry [12,22,29].

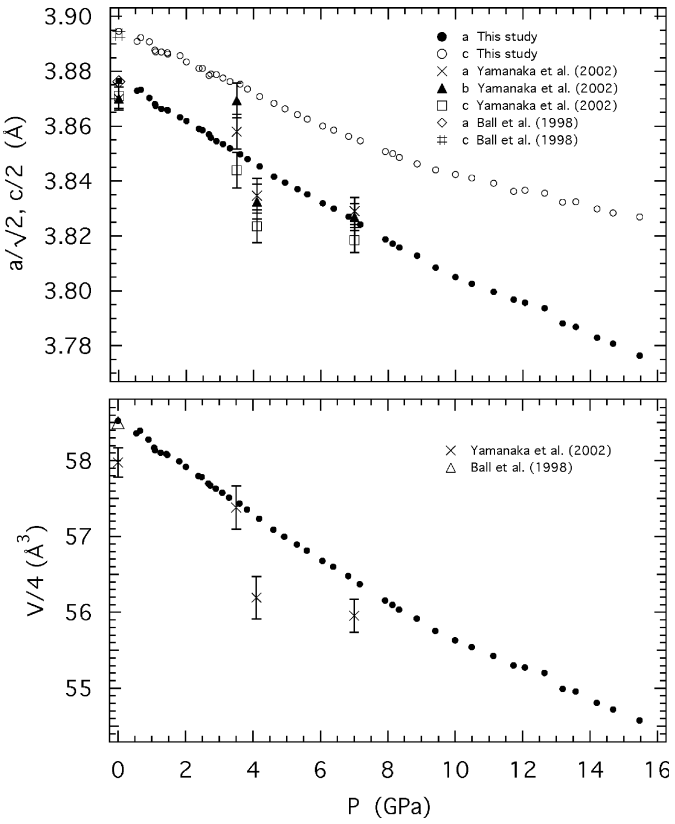

Fig. 5. Variations of pseudo-cubic lattice parameters ($a/\sqrt{2}$, $c/2$, $V/4$) of the refined tetragonal structure. Uncertainties ($\pm 1\sigma$ from the refinements) are smaller than the size of the symbols. Small discontinuities are evident close to 1 and 13 GPa, and a break in slope possibly occurs in $c/2$ at ~3.5 GPa. Also shown are pseudo-cubic lattice parameters for samples with the same nominal composition from the literature [6,36]. The data of Ball et al. [6] are in close agreement with the ambient pressure data given here, while those from Table 3 of Yamanaka et al. [36] appear to be for a structure which more nearly has cubic lattice geometry.

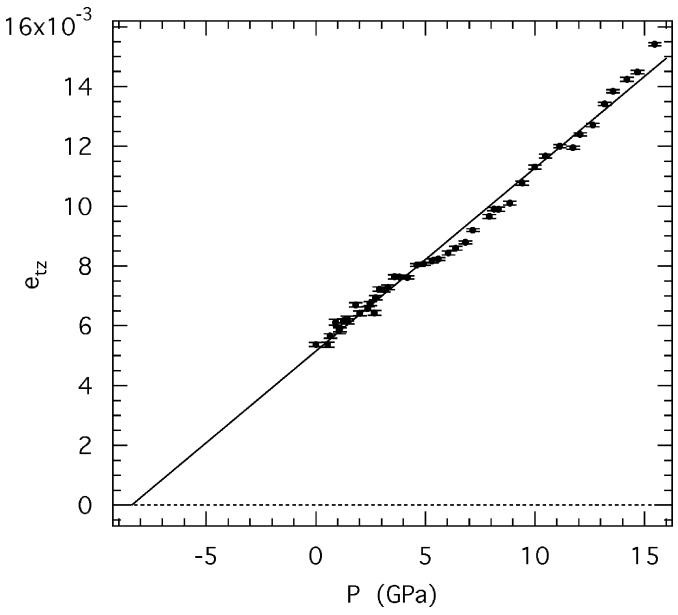

Fig. 6. Variation of the tetragonal strain, e_{tz}, determined from the lattice parameters given in Fig. 5. Error bars are propagated from $\pm 1\sigma$ for the individual lattice parameters. The straight line fit through all the data extrapolates to zero strain at −8.41 GPa. There is clearly a break in the trend of the pressure dependence of e_{tz} in the vicinity of 3–4 GPa.

Some new transition involving tetragonal or pseudo-tetragonal structures perhaps occurs in the vicinity of 3 GPa, but another possibility is simply that the strength of coupling between the volume strain, e_a, and q_4^2 (i.e the magnitude of the coupling coefficient λ_2) varies with pressure. If this coupling were constant, e_a of an $I4/mcm$ structure would vary as [13,45]

$$e_a = -\frac{\lambda_2 q_4^2}{\frac{1}{3}(C_{11}^o + 2C_{12}^o)}. \quad (9)$$

The critical pressure, P_c, and the evolution of q_4^2 are both sensitive to the value of λ_2 so that small variations of this coupling parameter would be expected to cause changes in the evolution of q_4^2 with pressure, as might then be observed as changes in the evolution of e_{tz}.

5. Comparison with elasticity data from pulse-echo ultrasonics

Carpenter et al. [37] have recently determined the bulk and shear moduli of a polycrystalline sample of $(Ca_{0.35}Sr_{0.65})TiO_3$ by conventional pulse-echo ultrasonic methods in situ at pressures up to ~11 GPa (data reproduced in Fig. 7a and b). The starting material was from the same batch of synthetic sample as used in the present study but it was hot pressed (7.5 GPa, 1000 °C) to produce a dense pellet. Hot pressing causes a change in colour from pale cream to black, which is interpreted as being due to reduction of a small percentage of Ti^{4+} to Ti^{3+} [52]. Classical phase transitions involving group–subgroup symmetry relations frequently show discontinuities in elastic constants at the transition point. Such discontinuities are not obvious in the data which, rather, show breaks in slope. The shear modulus, G, varies linearly with pressure but with different slopes above and below ~2–3 GPa. The evolution of the bulk modulus, K, is more complicated but perhaps also shows a break in slope (between non-linear segments) at about the same pressure.

Changes in the bulk modulus are expected to correlate with changes in volume strain, while changes in shear modulus might be reflected in changes of the shear strain, e_{tz}. Breaks in slope for both e_{tz} and G occur at about the same pressure as if there is a change in the strength of coupling between the tetragonal strain and the order parameter. A more quantitative comparison of the data for K and volume can be achieved through the use of the Murnaghan equation of state. If it is assumed that the bulk modulus varies linearly with pressure according to

$$K = K_o + K' \cdot P, \quad (10)$$

Table 1
Strain/order parameter relationships for selected strains in known octahedral tilting structures of the (Ca, Sr)TiO_3 system [13,45,48]

Space group	I4/mcm	Imma	Cmcm	Pnma
Order parameter components	$q_4 \neq 0$, $q_1 = q_2 = q_3 = q_5 = q_6 = 0$	$q_4 = q_6 \neq 0$, $q_1 = q_2 = q_3 = q_5 = 0$	$q_3 \neq 0$, $q_4 \neq 0$, $q_1 = q_2 = q_5 = q_6 = 0$	$q_2 \neq 0$, $q_4 = q_6 \neq 0$, $q_1 = q_3 = q_5 = 0$
Relationship to pseudo-cubic unit cell	$a = b = \sqrt{2}a_{pc}$ $c = 2c_{pc}$	$a = \sqrt{2}a_{pc}$ $b = 2b_{pc}$ $c = \sqrt{2}c_{pc}$	$a = 2a_{pc}$ $b = 2b_{pc}$ $c = 2c_{pc}$	$a = \sqrt{2}a_{pc}$ $b = 2b_{pc}$ $c = \sqrt{2}c_{pc}$
Orientation with respect to reference axes	c‖Z	b‖X	b‖Z	b‖X
Strain/order parameter relationship	$e_{tz} = -\frac{2\lambda_4 q_4^2}{(1/2)(C_{11}^o - C_{12}^o)}$	$e_{tx} = \frac{2\lambda_4 q_4^2}{(1/2)(C_{11}^o - C_{12}^o)}$	$e_{tz} = \frac{\lambda_3 q_3^2 - 2\lambda_4 q_4^2}{(1/2)(C_{11}^o - C_{12}^o)}$	$e_{tx} = \frac{2\lambda_4 q_4^2 - 2\lambda_3 q_2^2}{(1/2)(C_{11}^o - C_{12}^o)}$

The tetragonal strains e_{tz} and e_{tx} are defined with respect to linear strains e_1, e_2, e_3 as $e_{tz} = (1/\sqrt{3})(2e_3 - e_1 - e_2)$ and $e_{tx} = (1/\sqrt{3})(2e_1 - e_2 - e_3)$, respectively.

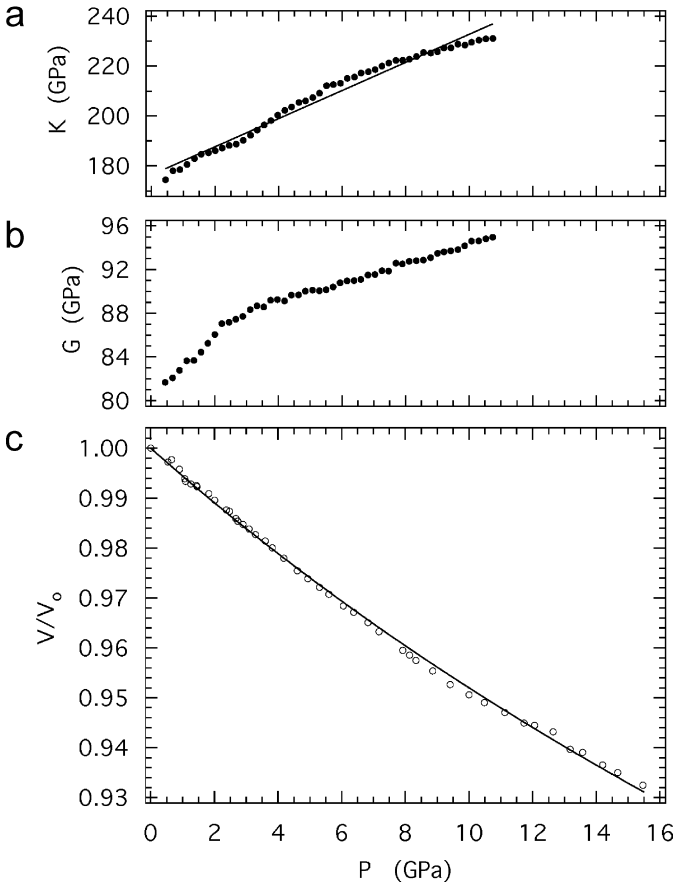

Fig. 7. (a) Bulk (K) and (b) shear (G) modulus variations for $(Ca_{0.35}Sr_{0.65})TiO_3$ perovskite obtained by pulse-echo ultrasonics (from [37]). The data for G show a break in slope between linear segments at ~2–3 GPa. The data for K are more variable but, perhaps, also show a break in slope between non-linear segments at ~3 GPa. The straight line is a linear least squares fit through all the data for K. (c) Murnaghan equation of state (solid line) for V/V_o, with $K_o = 176.4$ GPa and $K' = 5.6$ from the linear fit shown in (a), in comparison with the experimental data.

the unit cell volume would be expected to follow:

$$\frac{V}{V_o} = \left(1 + \frac{K' \cdot P}{K_o}\right)^{(-1/K')}, \quad (11)$$

where V_o is the unit cell volume at zero pressure (usually taken to be the ambient pressure value). A least squares fit to the data for K gives $K_o = 176.4(8)$ GPa and $K' = 5.6(1)$ (the straight line in Fig. 7a), which then gives the calculated variation of V/V_o shown in Fig. 7c. The overall behaviour of both K and V/V_o is reproduced but agreement between the experimental data and the fit or calculated variations is only semiquantititative. It should be noted, also, that the experimental data are adiabatic for K and isothermal for V/V_o. A more detailed analysis will require a better understanding of whether the small irregularities are due to structural phase transitions, changes in compression mechanism or simply to experimental error.

6. Discussion

In spite of the fact that $(Ca_{0.35}Sr_{0.65})TiO_3$ perovskite at room temperature is only ~5–10 K above the stability field of the *Pbcm* structure and not much more above the metastable extension of the stability field of the *Pnma* structure, no direct evidence has been found in this diffraction study for a tetragonal↔orthorhombic phase transition at high pressures. The sample remained tetragonal or, at least pseudo-tetragonal, at all pressures up to ~15.5 GPa. Subtle anomalies have been found in the evolution of the volume and the tetragonal strain, particularly near ~3 and ~13 GPa. No great significance can necessarily be assigned to the volume behaviour because deviations from the main trend are essentially at the level of noise in the data. On the other hand, the anomaly in tetragonal strain at 3–4 GPa coincides approximately with a break in slope of the independently determined shear modulus. These are, therefore, more likely to be real properties of the material. The additional weak reflections which appear in diffraction patterns collected in the pressure intervals 0.9–2.5 GPa and $P \geqslant 13.5$ GPa, the apparent change in FWHM at ~3 GPa and the abrupt change in the R-factor values at 2.5 GPa (Fig. 3a) are further indications that the sample could have undergone tetragonal↔tetragonal or tetragonal↔pseudo-tetragonal phase transitions at high pressures. It

should be stressed, however, that all the individual changes are small and that it has not yet been possible to identify positively the origin of the extra reflections. If the latter are not superlattice reflections of the perovskite, the breaks in slope of the shear parameters might imply simply that the sample displays small changes in compression mechanism. In this relatively low-pressure range, the methanol/ethanol medium is expected to deliver a hydrostatic pressure to the sample, with the implication that non-hydrostratic stress should not be a factor in the observed behaviour.

The present results differ from those reported by Yamanaka et al. [36] for a single crystal with the same nominal composition. One possibility, suggested by the pseudo-cubic lattice parameters which these authors report for both ambient conditions and high pressures, is that their sample had a slightly different Ca:Sr ratio and started in the stability field of the *Pbcm* structure. The samples were produced by different procedures and differences in oxygen or Ti contents between them might also be a factor.

Single-crystal diffraction data will be required to test the possibility that there is more than one (pseudo-) tetragonal structure for $(Ca_{0.35}Sr_{0.65})TiO_3$ perovskite at high pressure. If the extra reflections are indicative of a different superstructure, there are phase transitions at ~0.9, 2.5 and ~13 GPa. If it turns out that the structures at $0.9 < P < 2.5$ and $P \geqslant 13.5$ GPa are the same, the 13 GPa transition would be re-entrant. The critical parameters in determining such behaviour would be the coupling coefficients of the order parameter(s) with volume strain.

Acknowledgments

The sample used in this study was prepared as part of a separate project, with funding from the Natural Environment Research Council (Grant no. NER/A/S/2000/01055 to MAC). The ESRF is acknowledged for allocation of beam time to in-house research at ID27. SR acknowledges financial support from The Ministerio de Educacíon y Ciencia (Programa Ramón y Cajal).

References

[1] T. Mitsui, W.B. Westphal, Phys. Rev. 124 (1961) 1354–1359.
[2] J.G. Bednorz, K.A. Müller, Phys. Rev. Lett. 52 (1984) 2289–2292.
[3] T. Hirata, K. Ishioka, M. Kitajima, J. Solid State Chem. 124 (1996) 353–359.
[4] W. Kleemann, A. Albertini, M. Kuss, R. Lindner, Ferroelectrics 203 (1997) 57–64.
[5] V.V. Lemanov, Phys. Solid State 39 (1997) 1468–1473.
[6] C.J. Ball, B.D. Begg, D.J. Cookson, G.J. Thorogood, E.R. Vance, J. Solid State Chem. 139 (1998) 238–247.
[7] R. Ranjan, D. Pandey, V. Siruguri, P.S.R. Krishna, S.K. Paranjpe, J. Phys: Condens. Matter 11 (1999) 2233–2246.
[8] R. Ranjan, D. Pandey, J. Phys.: Condens. Matter 11 (1999) 2247–2258.
[9] S. Qin, A.I. Becerro, F. Seifert, J. Gottsmann, J. Jiang, J. Mater. Chem. 10 (2000) 1609–1615.
[10] R. Ranjan, D. Pandey, N.P. Lalla, Phys. Rev. Lett. 84 (2000) 3726–3729.
[11] R. Ranjan, D. Pandey, J. Phys: Condens. Matter 13 (2001) 4239–4249.
[12] R. Ranjan, D. Pandey, J. Phys: Condens. Matter 13 (2001) 4251–4266.
[13] M.A. Carpenter, A.I. Becerro, F. Seifert, Am. Miner. 86 (2001) 348–363.
[14] R. Ranjan, D. Pandey, W. Schuddinck, O. Richard, P. De Meulenaere, J. Van Landuyt, G. Van Tendeloo, J. Solid State Chem. 162 (2001) 20–28.
[15] C.J. Howard, R.L. Withers, B.J. Kennedy, J. Solid State Chem. 160 (2001) 8–12.
[16] R. Ouillon, J.-P. Pinan-Lucarre, P. Ranson, Ph. Pruzan, S.K. Mishra, R. Ranjan, D. Pandey, J. Phys.: Condens. Matter 14 (2002) 2079–2092.
[17] R.J. Harrison, S.A.T. Redfern, J. Street, Am. Miner. 88 (2003) 574–582.
[18] S.K. Mishra, R. Ranjan, D. Pandey, P. Ranson, R. Ouillon, J.-P. Pinan-Lucarre, P. Pruzan, J. Solid State Chem. 178 (2005) 2846–2857.
[19] P. Ranson, R. Ouillon, J.-P. Pinan-Lucarre, Ph. Pruzan, S.K. Mishra, R. Ranjan, J. Raman Spectrosc. 36 (2005) 898–911.
[20] C.J. Howard, R.L. Withers, Z. Zhang, K. Osaka, K. Kato, M. Takata, J. Phys.: Condens. Matter 17 (2005) L459–L465.
[21] S.K. Mishra, R. Ranjan, D. Pandey, H.T. Stokes, J. Phys.: Condens. Matter 18 (2006) 1885–1898.
[22] S.K. Mishra, R. Ranjan, D. Pandey, P. Ranson, R. Ouillon, J.-P. Pinan-Lucarre, P. Pruzan, J. Phys.: Condens. Matter 18 (2006) 1899–1912.
[23] D.I. Woodward, P.L. Wise, W.E. Lee, I.M. Reaney, J. Phys.: Condens. Matter 18 (2006) 2401–2408.
[24] R.A. Cowley, Phil. Trans. R. Soc. London A 354 (1996) 2799–2814.
[25] S.A.T. Redfern, J. Phys.: Condens. Matter 8 (1996) 8267–8275.
[26] B.J. Kennedy, C.J. Howard, B.C. Chakoumakos, J. Phys.: Condens. Matter 11 (1999) 1479–1488.
[27] R. Ali, M. Yashima, J. Solid State Chem. 178 (2005) 2867–2872.
[28] S.K. Mishra, R. Ranjan, D. Pandey, R. Ouillon, J.-P. Pinan-Lucarre, P. Ranson, Ph. Pruzan, Phys. Rev. B 64 (2001) 092302.
[29] S.K. Mishra, R. Ranjan, D. Pandey, B.J. Kennedy, J. Appl. Phys. 91 (2002) 4447–4452.
[30] T. Ishidate, S. Sasaki, K. Inoue, High Press. Res. 1 (1988) 53–65.
[31] T. Ishidate, T. Isonuma, Ferroelectrics 137 (1992) 45–52.
[32] B. Bonello, M. Fischer, A. Zarembowitch, Ultrasonics 27 (1989) 343–348.
[33] B. Bonello, M. Fischer, A. Polian, J. Acoust. Soc. Am. 86 (1989) 2257–2260.
[34] M. Fischer, B. Bonnello, A. Polian, J.-M. Léger, in: A. Navrotsky, D.J. Weidner, (Eds.), Perovskite: A Structure of Great Interest to Geophysics and Materials Science, vol. 45, Geophysical Monograph, 1989, pp. 125–130.
[35] A. Grzechnik, G.H. Wolf, P.F. McMillan, J. Raman Spectrosc. 28 (1997) 885–889.
[36] T. Yamanaka, N. Hirai, Y. Komatsu, Am. Miner. 87 (2002) 1183–1189.
[37] M.A. Carpenter, B. Li, R.C. Liebermann, Am. Miner. (2007) in press.
[38] M. Mezouar, W.A. Crichton, S. Bauchau, F. Thurel, H. Witsch, F. Torrecillas, G. Blattman, P. Marion, Y. Dabin, J. Chavanne, O. Hignette, C. Morawe, C. Borel, ESRF J. Synchrotron. Radiat. 12 (2005) 659–664.
[39] R. Le Toullec, J.P. Pinceaux, P. Loubeyre, High Press. Res. 1 (1988) 77–90.
[40] A.P. Hammersley, S.O. Svensson, M. Hanfland, A.N. Fitch, D. Häusermann, High Press. Res. 14 (1996) 235–248 A.P. Hammersley, ESRF Internal Report, ESRF98HA01T V9.129, 1998.
[41] R.A. Forman, G.J. Piermarini, J.D. Barnett, S. Block, Science 176 (1972) 284–285.

[42] A. Le Bail, H. Duroy, J.L. Fourquet, Mater. Res. Bull. 23 (1988) 447–452.
[43] J. Rodríguez-Caravajal, in: Abstracts of the Satellite Meeting on Powder Diffraction of the XV Congress of the IUCr, Toulouse, France, 1990, p. 127.
[44] G.J. Piermarini, S. Block, J.D. Barnett, J. Appl. Phys. 44 (1973) 5377–5382.
[45] M.A. Carpenter, Am. Miner. (2007) in press.
[46] M.A. Carpenter, Am. Miner. (2007) in press.
[47] S.A. Hayward, E.K.H. Salje, Phase Trans. 68 (1999) 501–522.
[48] M.A. Carpenter, C.J. Howard, B.J. Kennedy, K.S. Knight, Phys. Rev. B 72 (2005) 024118.
[49] ISOTROPY, H.T. Stokes, D.M. Hatch, Brigham Young University.
[50] M.A. Carpenter, C.J. Howard, K.S. Knight, Z. Zhang, J. Phys.: Condens. Matter (2006) in press.
[51] C.J. Howard, K.S. Knight, B.J. Kennedy, E.H. Kisi, J. Phys.: Condens. Matter 12 (2000) L677–L683.
[52] S. Webb, I. Jackson, J. Fitz Gerald, Phys. Earth Planet. Int. 115 (1999) 259–291.